

# Rain Fade Models

Subjects: Computer Science, Artificial Intelligence

Contributor: Feyisa Diba, Md Abdus Samad

Developing a rain fade model involves mathematical analysis of rain attenuation phenomena by reasoning and cause-based interaction.

Keywords: Earth–space link ; attenuation measurement ; microwave propagation ; rain fading ; rain attenuation

## 1. Introduction

Satellite communication is playing major role in the back-haul data network. In addition, satellite communication links can be used to enhance the existing telecommunication infrastructure in 5G and beyond networks [1][2][3], and satellite communication also has enormous applications for unmanned aerial vehicles (UAVs) and the Internet of Things (IoT) [4]. Because of radio congestion and broader bandwidth requirements, satellites switch to higher-frequency (33–75 GHz and 75–110 GHz) bands. However, atmospheric disturbances wreak havoc on these frequencies, causing attenuation, scintillation, and depolarization, lowering service efficiency [5]. Rain is one of the significant factors that creates attenuation on the propagation of electromagnetic waves. This effect has directed the interest of researchers in reducing the effect of rain on radio waves by controlling the transmitted power. Thus, multiple studies have been conducted on this globally. The research on rain attenuation is used to predict rain attenuation in various geographical areas over a wide range of frequency bands, especially for frequency bands over 10 GHz, and determine a suitable model that can predict attenuation. To develop such a model, the factors that impact attenuation first need to be determined. Some of the factors are related to the infrastructure setup (latitude, longitude, antenna size, antenna height, elevation angle, operating frequency) and some of them are related to the rain events such as wind flow, humidity, wind direction, and temperature.

It may be possible to evaluate the attenuation of atmospheric elements such as wind flow and the effect of the direction of wind flow on propagated signal attenuation separately, but it is conventional to consider attenuation due to other factors such as temperature, wind flow, and wind direction, along with rain attenuation. Even though rain attenuation issues were noticed in the middle of the last century, the problem has not yet been efficiently addressed. Besides the necessity to transfer a massive volume of data due to the fourth industrialization, the lower frequency bands are getting exhausted. This has led researchers to develop rain attenuation models that can work with higher frequency bands such as Q/V, W, and E-bands. For example, the application of a rain attenuation model for slant link, where the operating frequency is at 75 GHz, was assessed in [6][7]. Several models of rain attenuation have been proposed in the literature, and scientists are aiming to refine existing models for local climate conditions [8][9][10][11][12][13].

Precise rain attenuation determinations are critical for preparing the link budget, maintaining communication efficiency, and the architecture of the system. In addition, following probable rain attenuation determined by the rain attenuation model, the over- or underestimation of the power of the transmitter can be avoided. Radio-frequency engineers must comply with the permissible power transmission specifications in compliance with spectrum management rules for each frequency band. If the engineers do not follow such power regulations, the transmitted signal power may interfere with another frequency band, e.g., neighbor channel, which may disturb the neighboring telecommunication equipment. Thus, by deploying a rain attenuation model in Earth–space telecommunication, such disturbance can also be avoided. In the literature, there is currently a lack of survey papers addressing the issues and algorithms of slant link fade prediction models, which inspired us to write this survey paper. In [Table 1](#), some of the existing survey papers are presented, which are not adequate for covering the slant link fade prediction models.

**Table 1.** Rain attenuation survey papers.

Ref.	Survey Concentrations
[14]	<b>The results show that rain attenuation in horizontal polarization is slightly larger than that in vertical polarization. A differential coupling-based compensation was recommended to reduce the rain attenuation effects on polarization in the depolarization processes.</b>

Ref.	Survey Concentrations
[15]	In this survey, the artificial-neural-network-based models were classified based on input parameters. In addition, the accuracy of the artificial-neural-network-based models was accessed through a comparative study.
[16]	Rain attenuation in a satellite system is more severe than in a terrestrial system, and for a good model, it should be implemented into the model through local climatic elements.

## 2. Comparative Study of Slant Link Rain Fade Models

In the previous sections, we discussed the rain fade model prediction process. However, we may be interested in finding out some of the qualitative and quantitative characteristics of these models. Rain attenuation models for telecommunication links that support a wide variety of frequency spectra are a positive force. However, it is recommended to use a maximum 40 GHz frequency, as the next higher frequency band (above 40 GHz) may be used for astronomical and space communication purposes [17]. A 3–40 GHz frequency range is recommended for use in the telecommunication purposed Earth–space link to avoid possible interference with the deep-space communication link [18]. Table 2 presents the properties of slant link rain fade models such as whether they support terrestrial links; whether they consider rain structure including cloud, rainfall rate, frequency, elevation angle, rain layer height; and whether the models take into account the melting layer length within the effective path length. Table 3 shows the frequency spectrum supporting capabilities, the polarization used to evaluate the model, whether the model has a regional climatic parameter, whether the model considers rainfall rate distribution in a non-homogeneous means, and the recorded geographic area that suits the model properties. Table 4 shows whether these models were validated and the sources of rain attenuation related to measured databanks, constraints, and the complexity levels of the models in terms of low, medium, and high levels are classified. To validate the models, different validation tools such as the error figure and goodness-of-fit function, which is also known as relative error probability function, were mostly used [19][20][21]. Figure 2 shows the frequency range supporting capacity of the studied models. As we can see, the maximum frequency range supporting model is the unified model [22], the second highest is the Crane TC model [23], and the third top model is the GSST model [24]. The lowest frequency band supporting models from lowest to highest bands are Singapore [25], the Breakpoint model [26], the LU model [20], and the Karasawa model [27].

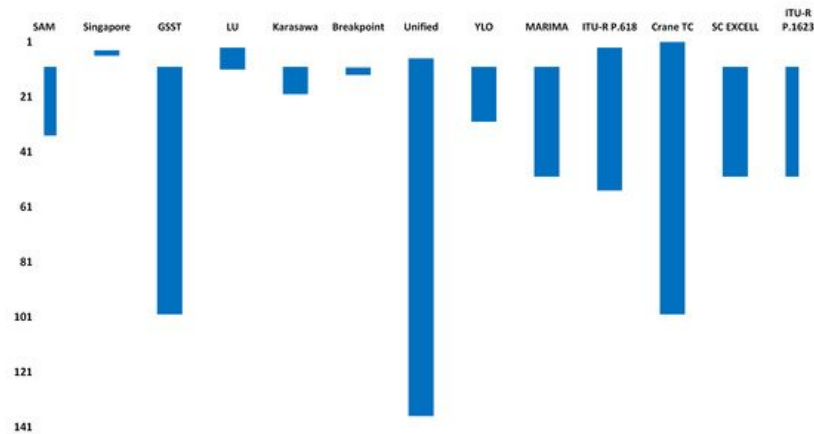


**Figure 2.** Each “vertical bar” represents the supported frequency range of the studied models. The vertical axis represents frequency in GHz and the horizontal axis represents the models.

**Table 2.** Characteristics table.

Tpe	Ref.	Slant or Both	Rain Structure	Rainfall Rate	Frequency	Angle(Earth Station)	Rain Height	Melting Layer Height	Time Series
EMPI	[28]	Slant	✓	✓	✓	✓	✗	✓	✓
	[25]	Slant	✗	✓	✓ ‡	✓ ^	✓	✗	✗
	[29]	Slant	✓	✓	✓	✓	✓	✗	✗
	[24]	Slant	✓	✓	✓	✓ ◊	✓	✓	✓
	[20]	Slant	✓ ◁	✗	✗	✗	✓	✓	✗
	[27]	Slant	✓	✓	✗	✓	✓ ▷	✗	✗
	[26]	Slant	✗	✓	✓ ‡	✓	✓	✗	✗
	[22]	Both	✗ ×	✓	✓	✓ ×	✗	✗	✗
	[12]	Slant	✗	✓	✓ ‡	✓ ‡	✓	✗ ×	✗
	[30]	Slant	✗	✓	✓ †	✗	✗	✗	✗
STAT	[31]	Slant	✗	✓	✓	✓	✓	✗	✓
	[32]	Slant	✗	✓	✓	✓	✓	✗	✗
	[33]	Slant	✗	✓	✓ ◊	✓ ◊	✗	✗	✗
	[34]	Slant	✗	✗ u	✗	✗	✗	✗	✓
	[35]	Slant	✓	✓	✓	✓	✓	✗	✗
PHY	[23]	Both	— >	✓	— ◻	✓	✓	✗	✗
	[36]	Both	✓ ◁	✓	✗	✓	✓	✓	✓
	[37]	Slant	✓	✓	✓	✓	✓	✓	✗
FADE	[38]	Slant	✗	✗	✓	✓	✗	✗	✗
	[39]	Slant	✗	✗	✗	✗	✗	✗	✓
	[40]	Slant	✗	✗	✓ ⊥	✓	✗	✗	✗
	[41]	Slant	✗	✗	— ⊕	✓ ⊖	✗	✗	✗
LB	[42]	Slant	✓	✓	✓	✓	✓	✓	✓

EMPI: empirical, STAT: statistical, PHY: physical, FADE: fade slope, LB: learning-based, ‡ k and  $\alpha$ , ^ 5–50°, ◊ 20–60°, ◁ ground layer and melting layer, ▷ exponential rain cell, × only rain height, no melting layer, × 6.50 72.8°. † as  $\alpha$  is dependent on frequency (not polarization), ◊ mentioned but no mathematical form is found, u rain attenuation is used, ◁ cylindrical rain cell, > the rain structure is composed of heavy and light rainfall components, ◻ frequency parameter is not directly used in the calculation of the attenuation, ⊥ as the applicable frequency range is limited to 10–50 GHz, ⊕ not mentioned, ⊖ s-constant that depends on elevation angle and climate.

**Table 3.** Characteristics table.

Type	Ref.	Frequency Range	Polarization	Regional Climatic Parameter	Spatial Friendly	Reported Region that Suits
	[28]	10–35 GHz	✓	✓	✓	The USA, Europe, and Japan
	[25]	4–6 GHz	NM ¶	Rainfall rate	✗	Singapore
	[29]	NM	✓	4 coefficient constants called a,b,c and d depend on geographic area	NM	Best suited areas are in Europe, the USA, Japan, and Australia
	[24]	10–100 GHz	✓Circular, horizontal and vertical	Rainfall rate	✗	Temperate region
EMPI	[20]	Above 11 GHz	✗	Local rainfall rate	No information available	No practical information; test information is limited within DBSG3 databank
	[27]	10–20 GHz	NM	Rainfall rate, the probabilities of occurrence and mean rainfalls, for cell and debris	The model considers a single volume rainfalling area and does not consider convective (cell) and stratified rain (debris)	CCIR rain zone
	[26]	10.7–13 GHz (Ku band)	✓	Rainfall rate	NM	Fiji
	[22]	Terrestrial: 7–137 GHz	✓k and α	Rainfall rate	✓	Worldwide (ITU-R databank)
	[12]	10–30 GHz	Both	Rainfall rate	✗	Tropical
	[30]	NM	✓	Rainfall rate	✗	Temperate region
	[31]	10–50 GHz	✓	Climate characteristics, link elevation angle	Has spatial dynamics of rainfall rate parameter due to Van de Kamp [43]	Xi'an, China
STAT	[32]	Up to 55 GHz	✓	Rainfall rate	✗	Worldwide
	[33]	NM (only 20 GHz is mentioned)	NM	NM	Information NM	France
	[34]	NM	✓Horizontal	Measured rain attenuation	NM	Kolkata, India
	[35]	Reported frequencies are 15, 30, 39.6 GHz	NM	✓	Rainfall rate is not a function of distance	Temperate and tropical
PHY	[23]	1–100 GHz	✗	Cell and debris parameter	No spatial correlation function is included	Temperate region
	[36]	11.6 GHz (Range NM)	✓Circular, Linear	Rainfall rate, wind velocity	✓(1-year rainfall rate PDF was used)	Italy
	[37]	10–50 GHz	✓	Rainfall rate; rain height; melting layer height, etc.	✓Vertical and horizontal	Worldwide
	[38]	Ku-band	RHCP, Linear polarization	✗	✗	Japan (low-elevation Earth-space path)
FADE	[39]	NM	Horizontal	✓	✗	Tropical area
	[40]	10–50 GHz	NM	✓ ⚡	✗	Designed for global perspective
	[41]	10.982 GHz (Ku-band)	Vertical	s-parameter □	✗	Malaysia

Type	Ref.	Frequency Range	Polarization	Regional Climatic Parameter	Spatial Friendly	Reported Region that Suits
LB	[42]	NM	NM	Local rainfall data: it needs to train the BPNN networks	NM	Butare, Rwanda

EMPI: empirical, STAT: statistical, PHY: physical, FADE: fade slope, LB: learning-based rain attenuation model, † not mentioned, ∞ elevation angle, □ s-parameter definition is given in Equation (60).

**Table 4.** Characteristics table.

Type	Ref.	Used/Validation Databank	Remarks about Validation	Complexity Level	Constraints
	[28]	62 experiments in the USA, Japan and Europe	Shows better prediction with minimum 2 years rainfall datasets	low	The operating frequency range is limited to 10–35 GHz
	[25]	INTELSAT POR experiment (Singapore)	The results have been validated with CCIR model and measured attenuation	low	The recommended frequency is limited to 4–6 GHz
	[29]	77 satellite links placed in Europe, the USA, Japan, and Australia (CCIR data bank)	Validated by the author	low	The model is suitable for prediction with an elevation angle ranging from 10° to 40°
	[24]	ITU-R databank	ITU-R databank is used to examine the behavior of m parameter at different frequencies as well as different sites	low	Not spatial friendly
EMPI	[20]	DBSG3 databank	The RMS value show that the new model provides the smallest rms and STD in all percentages of time except at 0.001%	high	Application area is limited by low latitudes (between 36° South and 36° North) and low elevation angles (25° <)
	[27]	CCIR rain zone with different elevation angle	Validated by the author	medium +	10–20 GHz
	[26]	Used 6 tropical city's rain databanks from ITU-R	The experimental result agreed about correction factor induced attenuation especially at elevation angle less than 60° compared to ITU-R model	medium	In this model it is assumed that rain is uniformly distributed inside a rain cell
	[22]	ITU-R databank	The model gives decent results with the correctness of its terrestrial and slant direction	medium	The model was not checked with actual data for attenuation
	[12]	×	Verified with the the beacon signals from WINDS and GE23 satellites (2009 to 2012)	low	Up to 30 GHz frequency is examined

Type	Ref.	Used/Validation Databank	Remarks about Validation	Complexity Level	Constraints
STAT	[30]	X	Not validated with heavy rainfall or with rainfall data around the world for different sites	low	The model is applicable only during the rain periods because no transition is included in the model to switch from rainy to clear sky conditions
	[31]	Validated based on the measured rain attenuation data at Xi'an, China	The validation is a good agreement between measured and predicted attenuation using this model, but has not been compared with other important rain attenuation models	high	The size of the area is not defined for a specific set of parameters
	[33]	X	Not validated	—	The probabilistic weather forecasts could be beneficial to maximize the economic value accounting the transmitted data for higher frequencies (say 50 GHz).
	[34]	X: used measured attenuation data	The validation shows a good agreement between measured and predicted attenuation using this model, but has not been compared with other important rain attenuation models	medium	It needs to derive mean and standard deviation of the Gaussian distribution for a different geographic area and find the coefficients of second-order polynomials from real measured attenuation
	[35]	✓	Validated at Lae, Papua New Guinea	low	—
PHY	[23]	Satellite: validated through CCIR procedure. Terrestrial: 35 terrestrial paths around the world	Both satellite and terrestrial links have been verified	high †	The probabilities of incidence and mean precipitation for cells and debris are difficult to determine
	[36]	Experimental dataset	The experimental results show that the method show less error probability.	medium	Needs 1 min rainfall rate
	[37]	DBSG3 databank	Although the model does not outperform the existing ITU-R model (approximately 2.4% error), it supports a few additional facilities (e.g., site diversity) and takes account of the interference due to hydrometer scattering	high	The correctness is limited by the local values of input parameters like the melting layer and the rain plateau value, which might not be available everywhere
	[38]	Experimental dataset	Validated with	low	—
	[39]	X	Validated in Kolkata, India, with experimental set-up	low	To use fade margin data it needs to remove tropospheric scintillation
FADE	[41]	Only experimental dataset	The resulted output agrees with the measured standard deviation of attenuation	low	The method was tested only at 10.982 GHz
	[40]	NM	Validated in [44][45]	low	Applicable for limited elevation angle 5–60°
LB	[42]	Durban, South Africa	The model was not validated with standard DSDB3 or CCIR rain databanks	—	The model was not tested with established well-known rain databanks like DBSG3 or CCIR

EMPI: empirical, STAT: statistical, † it needs to solve at least seven equations. PHY: physical, FADE: fade slope, LB: learning-based rain attenuation model, † it needs to solve ten equations.

## References

1. Evans, B.; Wang, N.; Rahulan, Y.; Kumar, S.; Cahill, J.; Kavanagh, M.; Watts, S.; Chau, D.K.; Begassat, Y.; Brunel, A.P.; et al. An integrated satellite-terrestrial 5G network and its use to demonstrate 5G use cases. *Int. J. Satell. Commun. Netw.* 2021.
2. Goratti, L.; Herle, S.; Betz, T.; Garriga, E.T.; Khalili, H.; Khodashenas, P.S.; Brunel, A.P.; Chau, D.K.; Ravuri, S.; Vasudevamurthy, R.; et al. Satellite integration into 5G: Accent on testbed implementation and demonstration results for 5G Aero platform backhauling use case. *Int. J. Satell. Commun. Netw.* 2020.
3. Strinati, E.C.; Barbarossa, S.; Choi, T.; Pietrabissa, A.; Giuseppi, A.; Santis, E.D.; Vidal, J.; Becvar, Z.; Haustein, T.; Cassiau, N.; et al. 6G in the sky: On-demand intelligence at the edge of 3D networks (Invited paper). *ETRI J.* 2020, 42, 643–657.
4. Marchese, M.; Moheddine, A.; Patrone, F. IoT and UAV Integration in 5G Hybrid Terrestrial-Satellite Networks. *Sensors* 2019, 19, 3704.
5. Cuervo, F.; Martín-Polegre, A.; Las-Heras, F.; Vanhoenacker-Janvier, D.; Flávio, J.; Schmidt, M. Preparation of a CubeSat LEO radio wave propagation campaign at Q and W bands. *Int. J. Satell. Commun. Netw.* 2020.
6. Badron, K.; Ismail, A.F.; Din, J.; Tharek, A. Rain induced attenuation studies for V-band satellite communication in tropical region. *J. Atmos. Sol. Terr. Phys.* 2011, 73, 601–610.
7. Norouzian, F.; Marchetti, E.; Gashinova, M.; Hoare, E.; Constantinou, C.; Gardner, P.; Cherniakov, M. Rain Attenuation at Millimeter Wave and Low-THz Frequencies. *IEEE Trans. Antennas Propag.* 2020, 68, 421–431.
8. Kalaivaanan, P.M.; Sali, A.; Abdullah, R.S.A.R.; Yaakob, S.; Singh, M.J.; Al-Saegh, A.M. Evaluation of Ka-Band Rain Attenuation for Satellite Communication in Tropical Regions Through a Measurement of Multiple Antenna Sizes. *IEEE Access* 2020, 8, 18007–18018.
9. Abdulrahman, A.Y.; Rahman, T.A.; Rafiqul, I.M.; Olufeagba, B.J.; Abdulrahman, T.A.; Akanni, J.; Amuda, S.A.Y. Investigation of the unified rain Attenuation prediction method with data from tropical Climates. *IEEE Antennas Wirel. Propag. Lett.* 2014, 13, 1108–1111.
10. Khairolanuar, M.; Ismail, A.; Badron, K.; Jusoh, A.; Islam, M.; Abdullah, K. Assessment of ITU-R predictions for Ku-Band rain attenuation in Malaysia. In *Proceedings of the 2014 IEEE 2nd International Symposium on Telecommunication Technologies (ISTT)*, Langkawi, Malaysia, 24–26 November 2014; pp. 389–393.
11. Chodkaveekityada, P. Comparison of spatial correlation between Japan and Thailand. In *Proceedings of the 2017 International Symposium on Antennas and Propagation (ISAP)*, Phuket, Thailand, 30 October–2 November 2017; pp. 1–2.
12. Yeo, J.X.; Lee, Y.H.; Ong, J.T. Rain Attenuation Prediction Model for Satellite Communications in Tropical Regions. *IEEE Trans. Antennas Propag.* 2014, 62, 5775–5781.
13. Lam, H.; Luini, L.; Din, J.; Capsoni, C.; Panagopoulos, A. Application of the SC EXCELL model for rain attenuation prediction in tropical and equatorial regions. In *Proceedings of the 2010 IEEE Asia-Pacific Conference on Applied Electromagnetics (APACE)*, Port Dickson, Malaysia, 9–11 November 2010; pp. 1–6.
14. Okamura, S.; Oguchi, T. Electromagnetic wave propagation in rain and polarization effects. *Proc. Jpn. Acad. Ser. B* 2010, 86, 539–562.
15. Samad, M.A.; Choi, D.Y. Learning-Assisted Rain Attenuation Prediction Models. *Appl. Sci.* 2020, 10, 6017.
16. Choi, K.S.; Kim, J.H.; Ahn, D.S.; Jeong, N.H.; Pack, J.K. Trends in Rain Attenuation Model in Satellite System. In *Proceedings of the 13th International Conference on Advanced Communication Technology (ICACT2011)*, Gangwon, Korea, 13–16 February 2011; pp. 1530–1533.
17. The European Space Agency. Satellite Frequency Bands. Available online: (accessed on 20 March 2021).
18. Report ITU-R SA.2167: Factors Affecting the Choice of Frequency Bands for Space Research Service Deep-Space (Space-to-Earth) Telecommunication Links; Report; International Telecommunication Union: Geneva, Switzerland, 2009.
19. Samad, M.A.; Diba, F.D.; Choi, D.Y. A Survey of Rain Attenuation Prediction Models for Terrestrial Links—Current Research Challenges and State-of-the-Art. *Sensors* 2021, 21, 1207.
20. Lu, C.S.; Zhao, Z.W.; Wu, Z.S.; Lin, L.K.; Thiennviboon, P.; Zhang, X.; Lv, Z.F. A New Rain Attenuation Prediction Model for the Earth-Space Links. *IEEE Trans. Antennas Propag.* 2018, 66, 5432–5442.
21. P.311-17: Acquisition, Presentation and Analysis of Data in Studies of Radiowave Propagation; Report; International Telecommunication Union: Geneva, Switzerland, 2017.

22. da Silva Mello, L.A.R.; Pontes, M.S. Improved unified method for the prediction of rain attenuation in terrestrial and earth space links. In Proceedings of the 2009 SBMO/IEEE MTT-S International Microwave and Optoelectronics Conference (IMOC), Belem, Brazil, 3–6 November 2009.
23. Crane, R.K. A two-component rain model for the prediction of attenuation statistics. *Radio Sci.* 1982, 17, 1371–1387.
24. Matricciani, E. Global formulation of the Synthetic Storm Technique to calculate rain attenuation only from rain rate probability distributions. In Proceedings of the 2008 IEEE Antennas and Propagation Society International Symposium, San Diego, CA, USA, 5–11 July 2008.
25. Ong, J. Rain rate and attenuation prediction model for Singapore. In Proceedings of the Ninth International Conference on Antennas and Propagation (ICAP), Eindhoven, The Netherlands, 4–7 April 1995.
26. Ramachandran, V.; Kumar, V. Modified rain attenuation model for tropical regions for Ku-Band signals. *Int. J. Satell. Commun. Netw.* 2006, 25, 53–67.
27. Yamada, M.; Karasawa, Y.; Yasunaga, M.; Arbesser-Rastburg, B. An improved prediction method for rain attenuation in satellite communications operating at 10–20 GHz. *Radio Sci.* 1987, 22, 1053–1062.
28. Stutzman, W.L.; Yon, K.M. A simple rain attenuation model for earth-space radio links operating at 10–35 GHz. *Radio Sci.* 1986, 21, 65–72.
29. Garcia-Lopez, J.; Hernando, J.; Selga, J. Simple rain attenuation prediction method for satellite radio links. *IEEE Trans. Antennas Propag.* 1988, 36, 444–448.
30. Maseng, T.; Bakken, P. A Stochastic Dynamic Model of Rain Attenuation. *IEEE Trans. Commun.* 1981, 29, 660–669.
31. Gong, S.; Gao, Y.; Shi, H.; Zhao, G. A practical MGA-ARIMA model for forecasting real-time dynamic rain-induced attenuation. *Radio Sci.* 2013, 48, 208–225.
32. P.618-13: Propagation Data and Prediction Methods Required for the Design of Earth-Space Telecommunication Systems; Report; International Telecommunication Union: Geneva, Switzerland, 2017.
33. Dahman, I.; Arbogast, P.; Jeannin, N.; Benammar, B. Rain attenuation prediction model for satellite communications based on the Météo-France ensemble prediction system PEARP. *Nat. Hazards Earth Syst. Sci.* 2018, 18, 3327–3341.
34. Das, D.; Maitra, A. Time series prediction of rain rate during rain events at a tropical location. *IET Microw. Antennas Propag.* 2012, 6, 1710–1716.
35. Bryant, G.H.; Adimula, I.; Riva, C.; Brussaard, G. Rain attenuation statistics from rain cell diameters and heights. *Int. J. Satell. Commun.* 2001, 19, 263–283.
36. Matricciani, E. Physical-mathematical model of the dynamics of rain attenuation based on rain rate time series and a two-layer vertical structure of precipitation. *Radio Sci.* 1996, 31, 281–295.
37. Capsoni, C.; Luini, L.; Paraboni, A.; Riva, C.; Martellucci, A. A New Prediction Model of Rain Attenuation that Separately Accounts for Stratiform and Convective Rain. *IEEE Trans. Antennas Propag.* 2009, 57, 196–204.
38. Karasawa, Y.; Matsudo, T. Characteristics of fading on low-elevation angle Earth-space paths with concurrent rain attenuation and scintillation. *IEEE Trans. Antennas Propag.* 1991, 39, 657–661.
39. Das, D.; Maitra, A. Time series prediction of rain attenuation from rain rate measurement using synthetic storm technique for a tropical location. *AEU Int. J. Electron. Commun.* 2014, 68, 33–36.
40. ITU-R Recommendations. P.1623: Prediction Method of Fade Dynamics on Earth-Space Paths; Report; International Telecommunication Union: Geneva, Switzerland, 2005.
41. Dao, H.; Islam, M.R.; Al-Khateeb, K.A.S. Rain Fade Slope Model in Satellite Path Based on Data Measured in Heavy Rain Zone. *IEEE Antennas Wirel. Propag. Lett.* 2013, 12, 50–53.
42. Ahuna, M.N.; Afullo, T.J.; Alonge, A.A. Rain Attenuation Prediction Using Artificial Neural Network for Dynamic Rain Fade Mitigation. *SAIEE Afr. Res. J.* 2019, 110, 11–18.
43. van de Kamp, M. Statistical analysis of rain fade slope. *IEEE Trans. Antennas Propag.* 2003, 51, 1750–1759.
44. Jong, S.L.; Riva, C.; D'Amico, M.; Lam, H.Y.; Yunus, M.M.; Din, J. Performance of synthetic storm technique in estimating fade dynamics in equatorial Malaysia. *Int. J. Satell. Commun. Netw.* 2018, 36, 416–426.
45. del Pino, P.G.; Riera, J.; Benarroch, A. Fade and interfade duration statistics on an Earth-space link at 50 GHz. *IET Microw. Antennas Propag.* 2011, 5, 790.

